

Supporting Information

Rapid Synthesis of Doped Metal Oxides via Joule-heating for Oxygen Electrocatalysis Regulation

Yajing Li^a, Han Wu^a, Jinfeng Zhang^a, Qi Lu^a, Xiaopeng Han^a, Xuerong Zheng^{a,b}, Yida Deng^{*a,b} and Wenbin Hu^{a,c}

^aSchool of Materials Science and Engineering, Tianjin Key Laboratory of Composite and Functional Materials, Key Laboratory of Advanced Ceramics and Machining Technology, (Ministry of Education), Tianjin University, Tianjin 300350, P. R. China

^bState Key Laboratory of Marine Resource Utilization in South China Sea, School of Materials Science and Engineering, Hainan University, Haikou 570228, P. R. China.

^cJoint School of National University of Singapore and Tianjin University International Campus of Tianjin University, Binhai New City, Fuzhou 350207, P. R. China

*Corresponding author. E-mail: yida.deng@tju.edu.cn

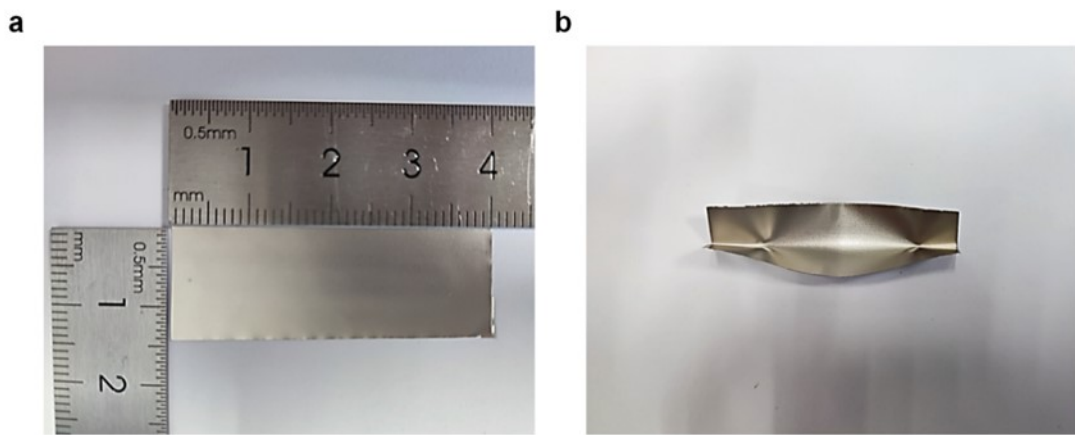


Fig. S1 (a-b) Photographs of Nickel foil ($4\text{ cm} \times 1.4\text{ cm} \times 0.02\text{ mm}$) used for the Joule heating.

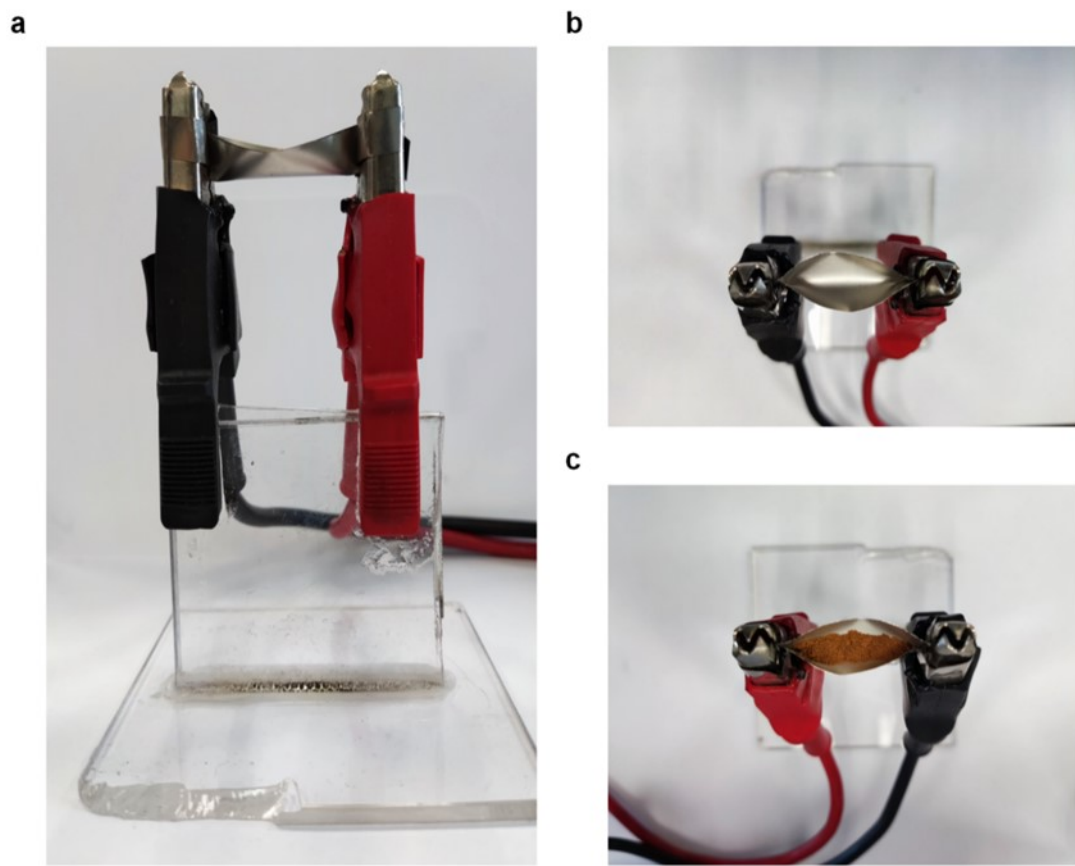


Fig. S2 (a-c) Photographs of clip used for the Joule heating.

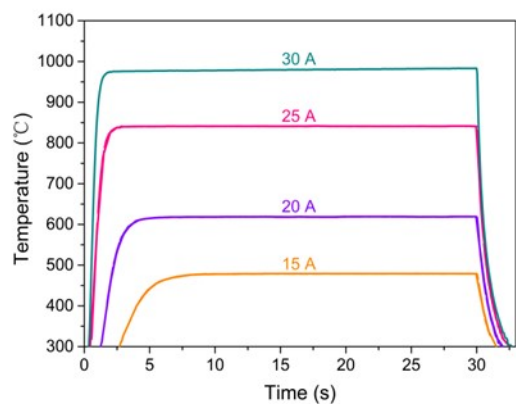


Fig. S3 Temperature curves of Joule heating at different currents (15 A, 20 A, 25 A, and 30 A).

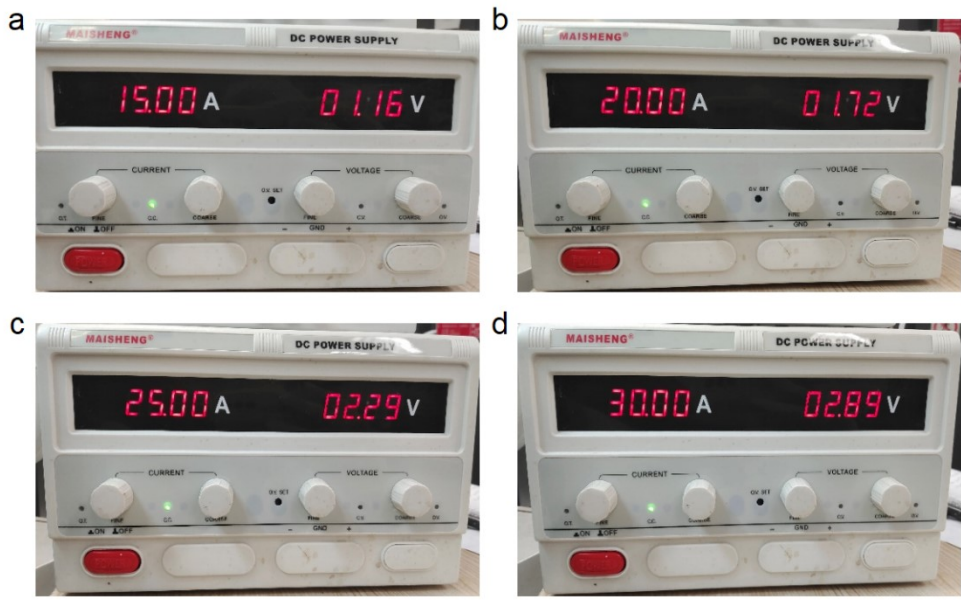


Fig. S4 (a-d) Photographs of the power supply under different voltage and current.

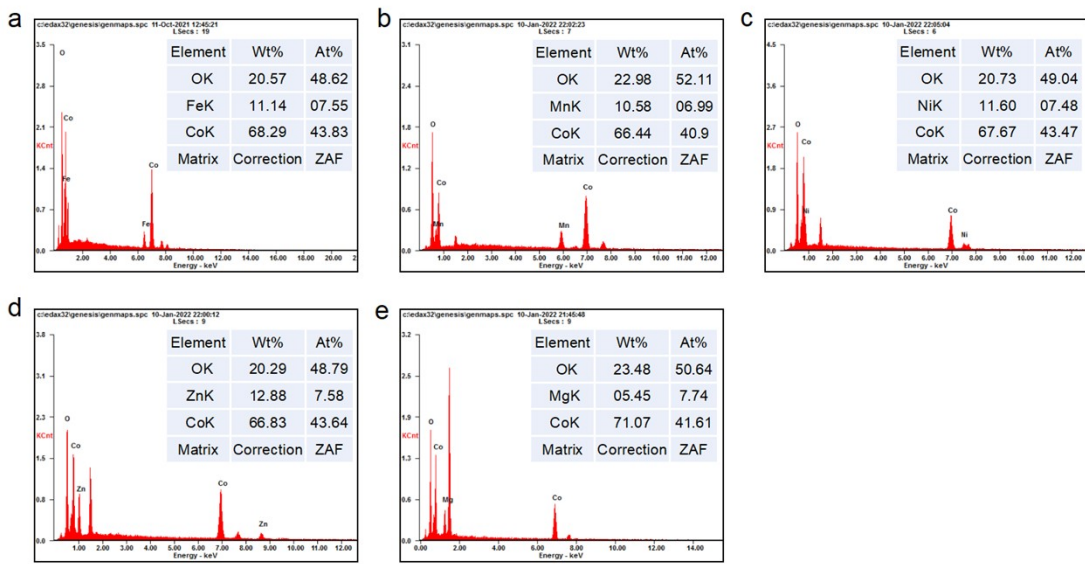


Fig. S5 EDS result (Insert: elemental ratio) of the synthesized Fe-CoO (a), Mn-CoO (b), Ni-CoO (c), Zn-CoO (d), and Mg-CoO (e) according to the EDS result.

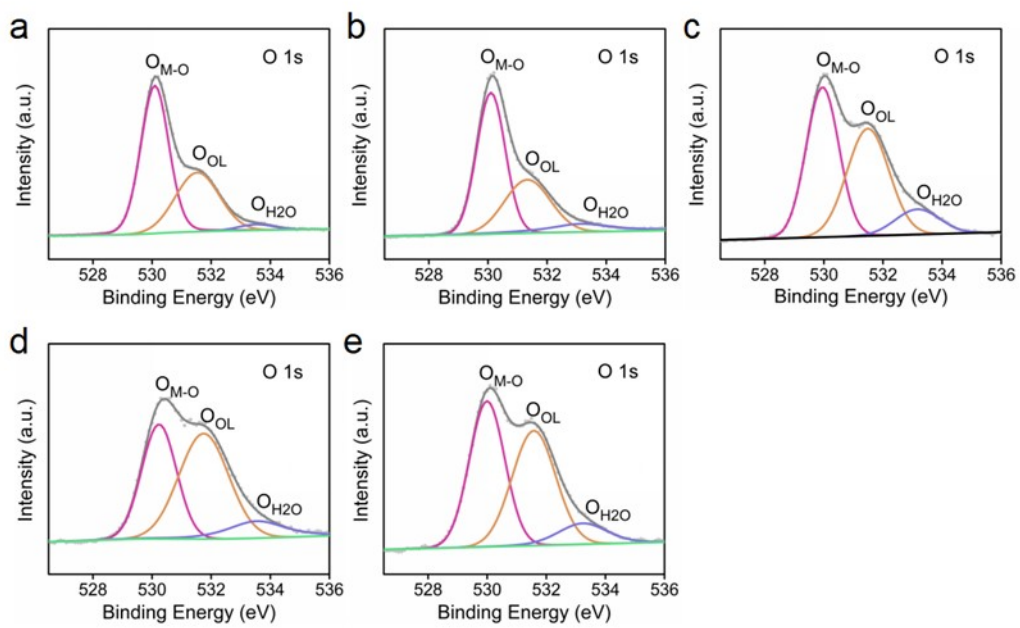


Fig. S6 O 1s XPS spectrum of Fe-CoO (a), Mn-CoO (b), Ni-CoO (c), Zn-CoO (d), and Mg-CoO (e).

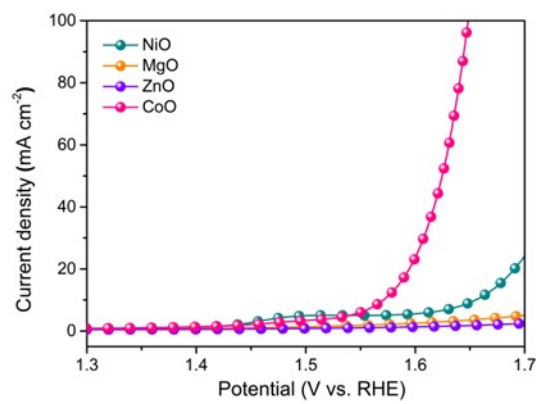


Fig. S7 LSV curves of the synthesized NiO, MgO, ZnO and CoO for OER.

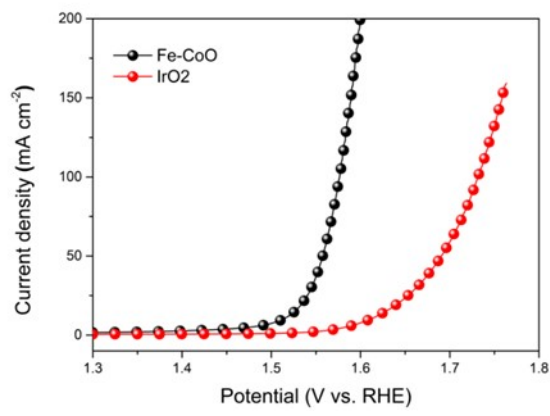


Fig. S8 LSV curves of the synthesized Fe-CoO and IrO₂ for OER.

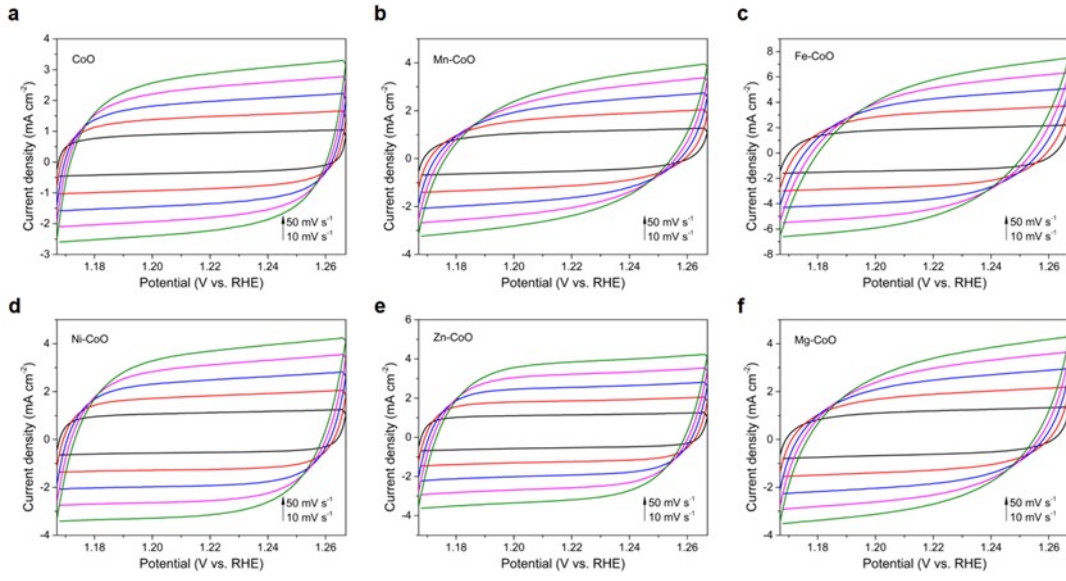


Fig. S9 CV curves from 10 mV s^{-1} to 50 mV s^{-1} of CoO (a), Mn-CoO (b), Fe-CoO (c), Ni-CoO (d), Zn-CoO (e), Mg-CoO (f).

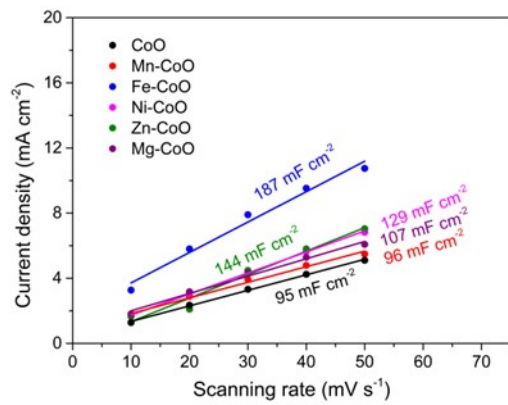


Fig. S10 Linear fitting of C_{dl} of CoO, Mn-CoO, Fe-CoO, Ni-CoO, Zn-CoO, Mg-CoO.

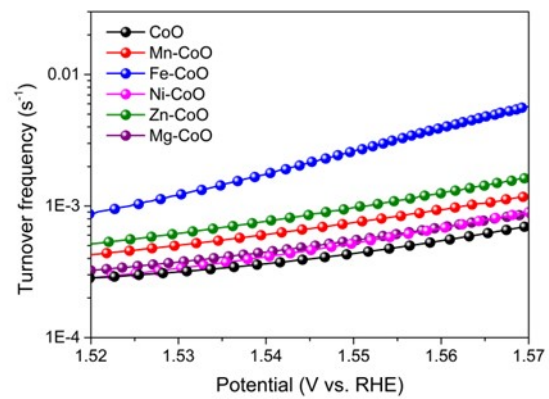


Fig. S11 TOF trends as a function of potential of CoO, Mn-CoO, Fe-CoO, Ni-CoO, Zn-CoO, Mg-CoO.

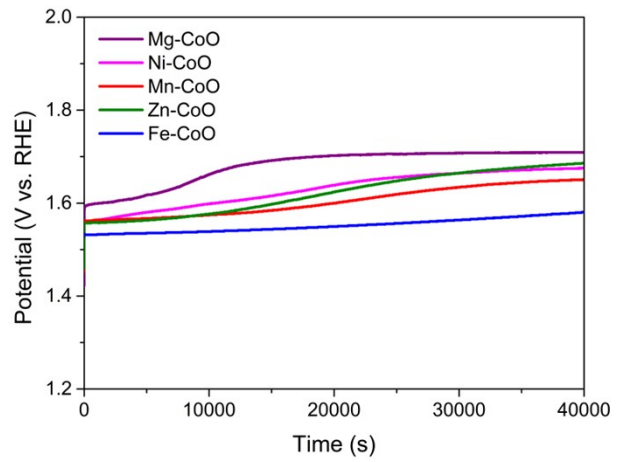


Fig. S12 OER stability tests of Fe-CoO, Mn-CoO, Ni-CoO, Zn-CoO, and Mg-CoO at a current density of 10 mA cm⁻².

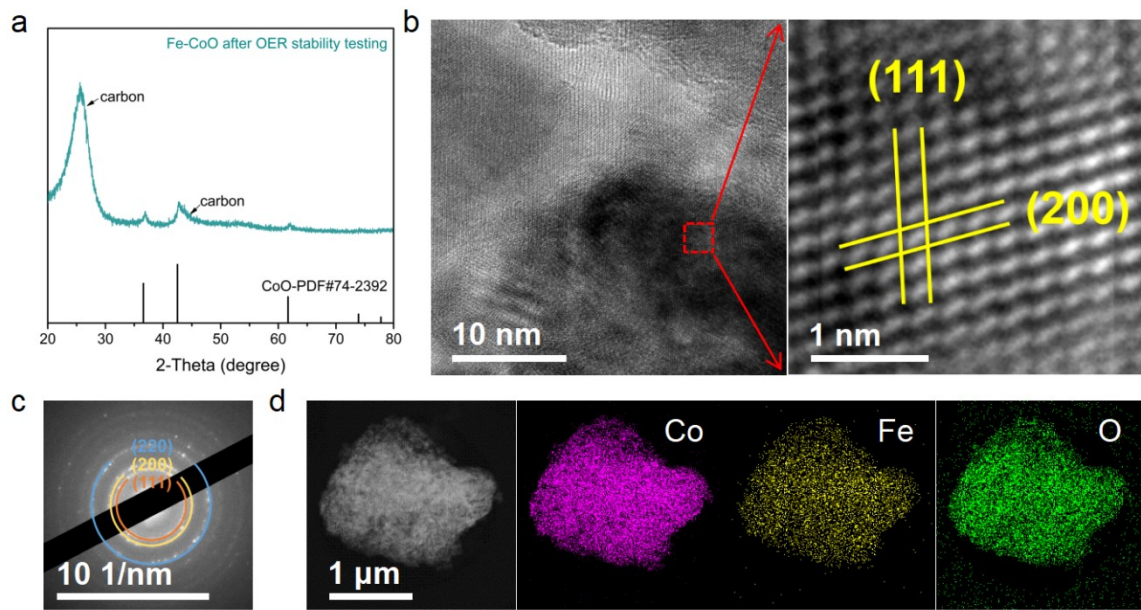


Fig. S13 XRD pattern (a), HRTEM image (b), diffraction pattern (c), and HAADF-STEM image and the corresponding elemental mapping distribution (d) of Fe-CoO after the OER stability test.

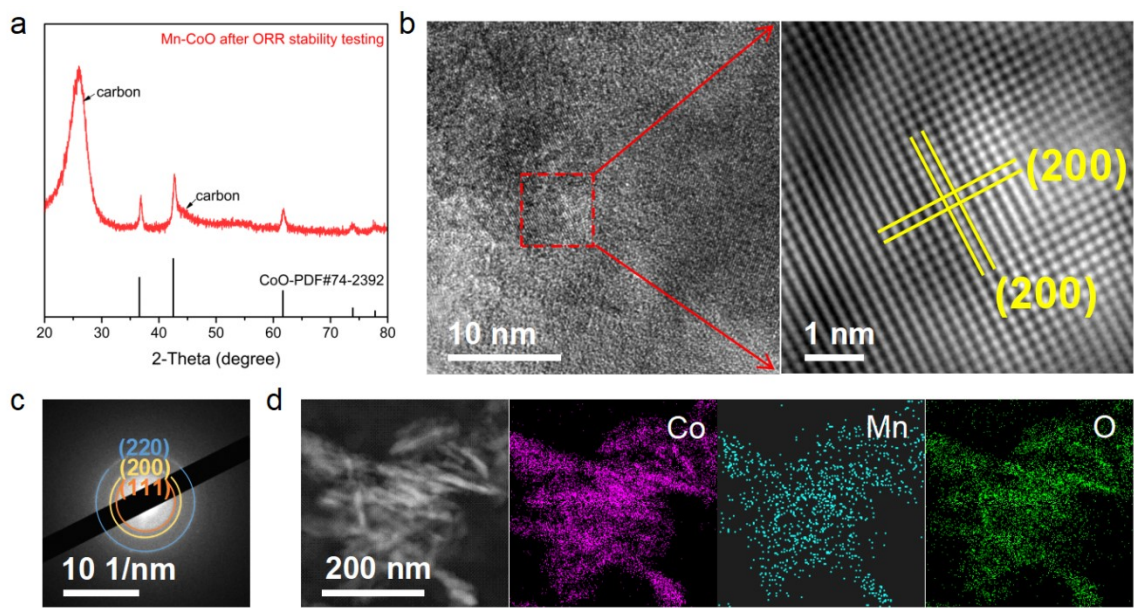


Fig. S14 XRD pattern (a), HRTEM image (b), diffraction pattern (c), and HAADF-STEM image and the corresponding elemental mapping distribution (d) of Mn-CoO after the OER stability test.

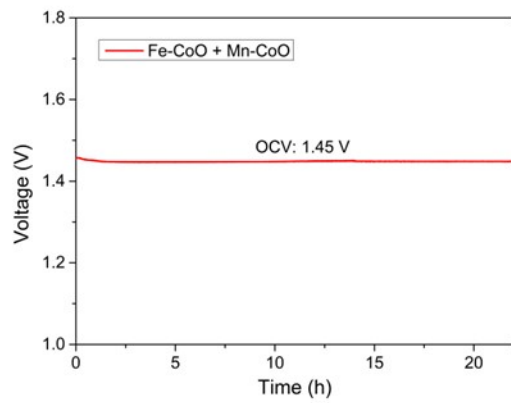


Fig. S15 Open-circuit voltage of AZAB with the mixed catalyst of Fe-CoO + Mn-CoO.

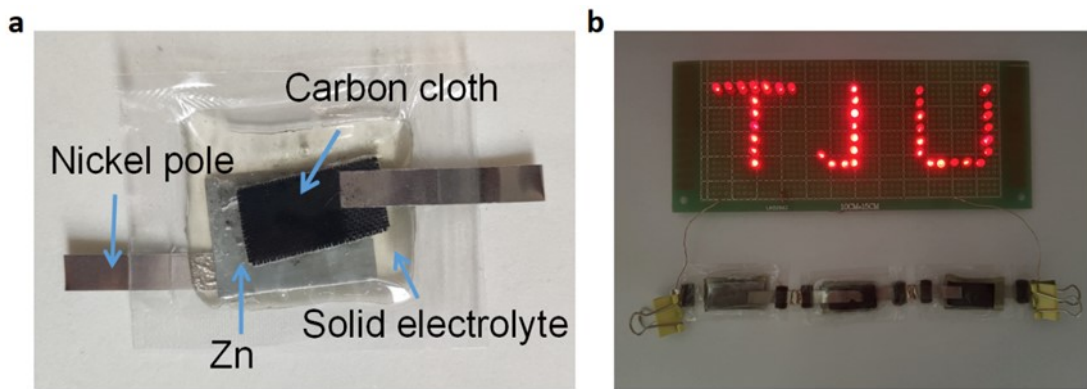


Fig. S16 (a) The photograph of the all-solid-state Zinc-air battery; (b) A LED screen that was powered by three Fe-CoO+Mn-CoO-based all-solid-state Zinc-air batteries.

Table S1 Metal activity order

Number	1	2	3	4	5	6	7	8	9	10
Element	Li	Cs	Rb	K	Ra	Ba	Fr	Sr	Ca	Na
Number	11	12	13	14	15	16	17	18	19	20
Element	La	Pr	Nd	Pm	Sm	Eu	Ac	Gd	Tb	Am
Number	21	22	23	24	25	26	27	28	29	30
Element	Y	Mg	Dy	Tm	Yb	Lu	Ce	Ho	Er	Sc
Number	31	32	33	34	35	36	37	38	39	40
Element	Pu	Th	Be	Np	U	Hf	Al	Ti	Zr	V
Number	41	42	43	44	45	46	47	48	49	50
Element	Mn	Nb	Zn	Cr	Ga	Fe	Cd	In	Ti	Co
Number	51	52	53	54	55	56	57	58	59	60
Element	Ni	Mo	Sn	Pb	H2	Cu	Po	Hg	Ag	Ru
Number	61	62	63	64	65					
Element	Os	Pd	Ir	Pt	Au					

Table S2 EIS fitting parameters from equivalent circuits for Fe-CoO, Mn-CoO, Ni-CoO, Zn-CoO, Mg-CoO, and CoO

Catalysts	Fe-CoO	Mn-CoO	Ni-CoO	Zn-CoO	Mg-CoO	CoO
R_s/Ω	1.9	1.76	1.84	1.92	1.95	1.81
R_{ct}/Ω	1.41	5.74	5.86	3.92	7.25	7.49

Table S3 Summary of the electrocatalytic and ZAB performances of recently reported electrocatalysts

Catalyst	OER Overpotential at 10 mA cm ⁻² vs. RHE (mV)	ORR Half-wave potential vs. RHE (V)	Electrolyte	Power density (mW cm ⁻²)	Durability Time (h)/current density (mA cm ⁻²)	Reference
Fe/Fe ₃ C-N-CNTs	290	0.83	6 M KOH	183	195/5	[1]
ZnCo ₂ @NCNTs-800	350	0.85	6 M KOH + 0.2 M Zn(OAc) ₂	194.3	311/5	[2]
Co _{0.25} Ni _{0.75} @NCNT	410	0.84	6 M KOH + 0.2 M Zn(OAc) ₂	167	36/5	[3]
NiCo-MOF@ZIF-L(Zn)	406	0.856	6 M KOH + 0.2 M Zn(OAc) ₂	163.7	more than 180 cycles at 2 mA cm ⁻²	[4]
Co-O-ZIF/PANI	351 at 50 mA cm ⁻²	0.7	6 M KOH + 0.2 M Zn(OAc) ₂	123.1	more than 300 cycles at 10 mA cm ⁻²	[5]
Co/CoS/Fe-HSNC	250	0.9	6 M KOH + 0.2 M Zn(OAc) ₂	213	50/2	[6]
Co ₃ O ₄ -Co@NC	350	0.86	6 M KOH + 0.2 M Zn(OAc) ₂	158	200/10	[7]
0.05CoO _x @PNC	320	0.88	6 M KOH + 0.2 M Zn(OAc) ₂	157.1	200/10	[8]
Co _x P@NPC	350	0.83	6 M KOH + 0.2 M Zn(OAc) ₂	157	140/10	[9]
FeCo-PC	—	—	—	61.3	70	[10]
Fe-CoO	280	—	—	—	—	this work
Mn-CoO	—	0.71	—	—	—	this work
Fe-CoO+Mn-CoO	—	—	6 M KOH + 0.2 M Zn(OAc) ₂	305	more than 450 cycles at 5 mA cm ⁻²	this work

Reference

1. L. Zong, X. Chen, S. Dou, K. Fan, Z. Wang, W. Zhang, Y. Du, J. Xu, X. Jia, Q. Zhang, X. Li, Y. Deng, Y. Chen and L. Wang, *Chinese Chemical Letters*, 2021, **32**, 1121-1126.
2. T. Qin, F. Li, X. Liu, J. Yuan, R. Jiang, Y. Sun, H. Zheng and A. P. O'Mullane, *Chem Eng J*, 2022, **429**, 132199.
3. A. Kundu, A. Samanta and C. R. Raj, *Acs Appl Mater Inter*, 2021, **13**, 30486-30496.
4. F. Wang, Y. Xu, Y. Wang, Z. Liang, R. Zhang, Y. Wang, H. Zhang, W. Zhang, R. Cao and H. Zheng, *Chem Commun*, 2021, **57**, 8190-8193.
5. H. Lei, S. Yang, Q. Wan, L. Ma, M. S. Javed, S. Tan, Z. Wang and W. Mai, *Journal of Energy Chemistry*, 2022, **68**, 78-86.
6. L. Yan, H. Wang, J. Shen, J. Ning, Y. Zhong and Y. Hu, *Chem Eng J*, 2021, **403**, 126385.
7. Z. Zhang, Y. Tan, T. Zeng, L. Yu, R. Chen, N. Cheng, S. Mu and X. Sun, *Nano Research*, 2021, **14**, 2353-2362.
8. Y. Tan, W. Zhu, Z. Zhang, W. Wu, R. Chen, S. Mu, H. Lv and N. Cheng, *Nano Energy*, 2021, **83**, 105813.
9. Q. Shi, Q. Liu, Y. Zheng, Y. Dong, L. Wang, H. Liu and W. Yang, *Energy & Environmental Materials*, 2022, **5**, 515-523.
10. Chen et al., Aqueous rechargeable zinc air batteries operated at -
110—————C, Chem (2022), <https://doi.org/10.1016/j.chempr.2022.10.028>.